Accepted Manuscript

Synthesis, anticancer, structural, and computational docking studies of 3-benzylchroman-4-one derivatives

Lalitha Simon, Abdul Ajees Abdul Salam, S. Madan Kumar, T. Shilpa, K.K. Srinivasan, K. Byrappa

PII: S0960-894X(17)31011-9
DOI: https://doi.org/10.1016/j.bmcl.2017.10.026
Reference: BMCL 25355

To appear in: *Bioorganic & Medicinal Chemistry Letters*

Received Date: 30 May 2017
Revised Date: 12 October 2017
Accepted Date: 13 October 2017

Please cite this article as: Simon, L., Salam, A.A.A., Madan Kumar, S., Shilpa, T., Srinivasan, K.K., Byrappa, K., Synthesis, anticancer, structural, and computational docking studies of 3-benzylchroman-4-one derivatives, *Bioorganic & Medicinal Chemistry Letters* (2017), doi: https://doi.org/10.1016/j.bmcl.2017.10.026

Synthesis, anticancer, structural, and computational docking studies of 3-benzylchroman-4-one derivatives

Lalitha Simon[a,†], Abdul Ajees Abdul Salam[b,†,*], Madan Kumar S[c], Shilpa T[b], Srinivasan, K.K[d], Byrappa K[e]

[a]Department of Chemistry, Manipal Institute of Technology, Manipal University, Manipal 576 104, India.

[b]Department of Atomic and Molecular Physics, Manipal University, Manipal 576 104, India.

[c]PURSE Lab, Mangalagangotri, Mangalore University, Mangalore 574 199, India.

[d]Department of Chemistry, Shri Madhwa Vadiraja Institute of Technology and Management, Vishwothama Nagar, Bantakal, Udupi - 576 115, India.

[e]Department of Material Science, Mangalagangotri, Mangalore University, Mangalore 574 199, India.

[†]These authors contributed equally to this study.

[*]**Corresponding Author:**

Department of Atomic and Molecular Physics,

Manipal University of Technology

Manipal University, Manipal 576 104,

Karnataka, India.

E-mail: abdul.ajees@manipal.edu

Phone: +91-8147966458.

Keywords: Benzylchroman-4-ones; Cytotoxicity; Single crystal; Molecular docking; MTT assay

Abstract:

A series of 3-Benzylchroman-4-ones were synthesized and screened for anticancer activity by MTT assay. The compounds were evaluated against two cancerous cell lines BT549 (human breast carcinoma), HeLa (human cervical carcinoma), and one noncancerous cell line vero (normal kidney epithelial cells). **3b** was found to be the most active molecule against BT549 cells (IC_{50} = 20.1 µM) and **3h** against HeLa cells (IC_{50} = 20.45 µM). **3b** also exhibited moderate activity against HeLa cells (IC_{50} = 42.8 µM). The molecular structures of **3h** and **3i** were solved by single crystal X-ray crystallographic technique. Additionally, the molecular

docking studies between the tumour suppressor protein p53 with the lead compound **3h**, which exhibited better anticancer activity against HeLa cells was examined.

Cancer is one of the most widespread and feared diseases in the world today. Cancer arises from the transformation of healthy cells into tumour cells in a multistage process that progresses from a pre-cancerous lesion to a malignant tumour. Cancer is the second leading cause of death globally and was responsible for 8.8 million deaths in 2015. Globally, nearly 1 in 6 deaths is due to cancer (http://www.who.int/mediacentre/factsheets/fs297/en/). Many cytotoxic drugs suffer from poor selectivity to target cells, leading to a high degree of toxicity and potentially life-threatening side effects. To design drugs that specifically target cancer cells is a major challenge. Flavonoids are shown to have anticancer activities.

3-Benzylchroman-4-ones (homoisoflavanones) are oxygen-containing heterocycles with a sixteen carbon skeleton. They belong to the class of naturally occurring polyphenolic flavonoids with limited occurrence in nature and are mainly found in families like Hyacinthaceae, Liliaceae, Agavaceae, Fabaceae, Liliaceae, and Polygonaceae.[1, 2] They have been reported to possess antiinflammatory, antibacterial, antihistaminic, antimutagenic, antiviral and angioprotective properties besides potent phosphodiesterase inhibition property.[3-5] Homoisoflavonoids, caesalpinianone, and 6-O-methylcaesalpinianone which exhibited different levels of glutathione S-transferase inhibitory and antifungal activities were isolated from the ethanolic extract of Caesalpinia bonduc (Fabaceae). Caesalpinanone and 6-O-methylcaesalpinianone inhibited glutathione S-transferase with an IC_{50} = 16.5 µM and 17.1 µM respectively.[6] Sappanone A, a homoisoflavanone isolated from the heartwood of Caesalpinia sappan has been known to have antioxidant and anti-inflammatory effects. A recent study showed that Sappanone A inhibited Cisplatin-induced kidney injury through activating Nrf2 and inhibiting NF-κB activation.[6] Pre-treatment with 5,7-dihydroxy-3-(3-hydroxy-4-methoxybenzyl)-chroman-4-one inhibited the production of intracellular ROS induced by UVB irradiation in HaCaT cells. Further analysis revealed a decrease in the level of MAPK activation and down-regulation of COX2 expression.5,7-dihydroxy-3-(3-hydroxy-4-methoxybenzyl)-6-methoxychroman-4-one inhibited vascular tube formation and new vessel growth induced by basic fibroblast growth factor.[7] Homoisopogon A (1), isolated from Ophiopogon japonicus tubers exhibited potent cytotoxicity against human lung adenocarcinoma LU-1, human epidermoid carcinoma KB, and human melanoma SK-Mel-2

cancer cells with IC_{50} values ranging from 0.51 to 0.66 µM.[8] However, reports on the anticancer activity of synthetic 3-benzyl-chromone derivatives are scarce. As part of our ongoing efforts to synthesize new flavonoids and explore their biological activities, we have synthesized 15 derivatives of 3-benzylchroman-4-one. Their anticancer potential is evaluated *in vitro* against two cancerous cell lines BT549 (human breast carcinoma), HeLa (human cervical carcinoma), and one non-cancerous cell line Vero (normal kidney epithelial cells). We also carried out the crystal structure of compounds **3h and 3i**. Moreover, we performed molecular docking studies of the tumour-suppressor protein p53 with a **3h** molecule, which shows better cytotoxic activity in HeLa cells.

3-Benzylchroman-4-one derivatives were synthesized as outlined in Scheme 1 and their chemical structures are summarized. Chalcones were synthesized by condensation of acetophenones/ methoxy/methyl substituted acetophenones and substituted aldehydes, using 40% w/v alcoholic KOH at room temperature.[9] Reduction of chalcones to dihydrochalcones was carried out using 10% Pd-C and ammonium formate.[10] The dihydrochalcones were then cyclized to the corresponding homoisoflavanones using paraformaldehyde and 50% v/v aqueous diethylamine.[11] The structures of derivatives **3a-o** were confirmed using elemental analysis, NMR spectroscopy and mass spectral analysis. For more details on experimental and complete NMR, and mass spectra see the supplementary data. Because of their wide range of pharmacological activity, we synthesized a series of 3-benylchroman-4-ones and evaluated their cytotoxic potential against two cell lines, BT549, and HeLa.

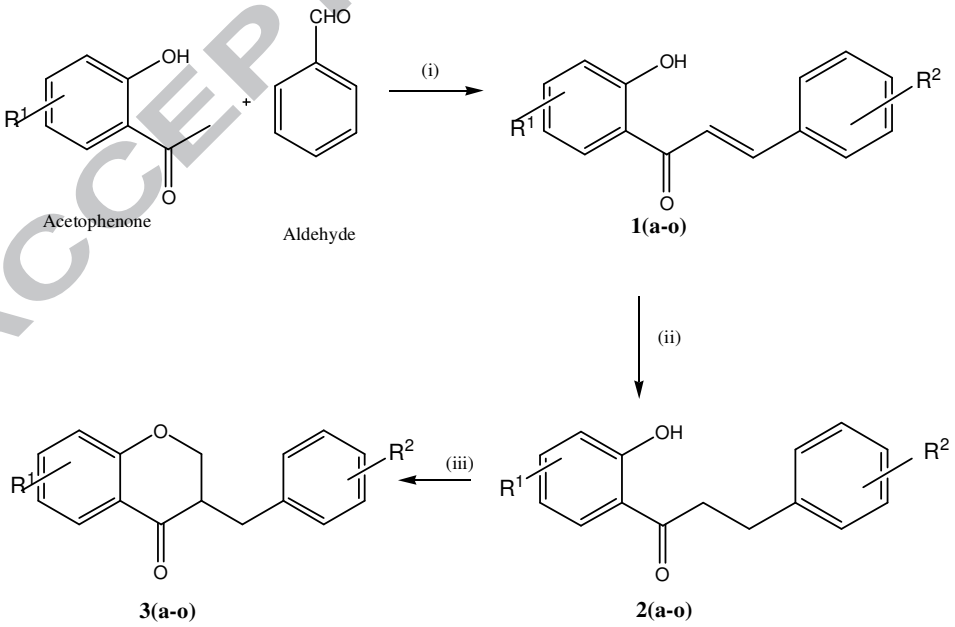

Compound	R^1	R^2
3a	H	4′-Cl
3b	H	4′-OH
3c	H	4′-F
3d	H	4′-OCH_3
3e	H	2′,3′,4′-OCH_3
3f	H	2′,4′-OCH_3
3g	H	3′,4′-OCH_3
3h	H	3′-OH,4′-OCH_3
3i	H	4′-CH_3
3j	6-CH_3	4′-OCH_3
3k	5-OCH_3	3′-OH,4′-OCH_3
3l	7-CH_3	4′-OCH_3
3m	7-CH_3	4′-OH
3n	7-OCH_3	4′-OH
3o	7-OCH_3	3′-OH,4′-OCH_3

Scheme 1. Synthesis of 3-Benzylchroman-4-one derivatives. Reagents and condition: (i) 40% w/v alcoholic KOH, rt, 12-36 h; (ii) 10% Pd-C, $HCOONH_4$, MeOH-THF (1:1), reflux, 90 min; (iii) 50% v/v aq. diethylamine, (HCHO)n, EtOH, reflux, 9 h.

The results of the *in vitro* anticancer activity of compounds **3a-o**, against BT549, HeLa, and Vero cells are listed in Table 1. **3b** was found to be the most active molecule against BT549 cells (IC_{50} = 20.1 µM) and **3h** against HeLa cells (IC_{50} = 20.45 µM). **3b** also exhibited moderate activity against HeLa cells (IC_{50} = 42.8 µM). The molecule 3b has hydroxyl substitution at C-4' of ring C, and **3h** has hydroxyl and methoxy substitutions at C'3 at C'4 of ring C respectively (Fig. 1). The compounds **3b**, **3m**, and **3n** have the same substitution (OH at C4') in ring B, but **3m** has a methyl group at C7 of ring A, and **3n** has a methoxy group at C7 of ring A. However the introduction of methyl group/methoxy group in ring A did not enhance the activity, instead slightly reduced it. Comparing the activities of **3d**, **3j** and **3l** we observed that having OCH_3 at C4' of ring B and no substitution in ring A or OCH3 at C4' of ring C and methyl function at C-6 of ring A led to decreased anticancer activity (IC_{50} > 100 µM). However, the compound **3l** with OCH_3 at C4' of ring C and methyl function at C7 of ring A showed moderate activity with IC_{50} = 42.12 µM, 68.32 µM against BT549 and HeLa cells respectively.

Table 1
Anticancer activities of 3a-o. The values are mean ± SEM of three independent triplicates. IC_{50} was determined by nonlinear regression using Graph Pad Prism v 5.03, CA, USA.

Compound	IC_{50} (µM)		
	BT 549	**HeLa**	**Vero**
3a	69.30 ±1.2	61.9 ±4.1	>200
3b	20.1 ± 0.9	42.8 ±2.7	>200
3c	>200	>200	>200
3d	>100	>100	>200
3e	>100	>100	>200
3f	61.90 ±5.8	38.26 ±1.3	>200
3g	>100	>100	>200
3h	>100	20.45 ±0.8	>200
3i	42.16 ±1.6	48.90 ±1.2	>200
3j	>100	76.3 ±2.5	>200
3k	>200	>200	>200
3l	42.12 ±4.8	68.32±6.5	>200
3m	28.7 ±07	43.01 ±4.0	>200
3n	24.3 ±3.2	50.38±1.8	>200
3o	30.6 ±1.4	50.12 ±1.1	>200

For derivatives bearing OH at C3' and OCH_3 at C4' of ring C (**3h, 3k, 3o**) **3h** showed significant activity against HeLa cells (IC_{50} = 20.45 µM). Furthermore, **3o** having a methoxy function at C7 of ring A showed moderate activity against both cell lines (IC_{50} = 39.4µM BT549, IC_{50} = 50.12µM HeLa). However, a methoxy function at C5 of ring A (**3k**) substantially decreased the activity (IC_{50} > 200µM). Considering halogen substitution at C4' of ring C, **3a** with chlorine at C4' was found to be active (IC_{50} = 69.3µM BT549, IC_{50} = 61.9µM HeLa) whereas **3c** with fluorine at C4' was found to be inactive (IC_{50} > 200µM). Furthermore, the molecule having methyl substitution at C4' of ring C, **3i** exhibited moderate anticancer activity against both cell lines (IC_{50} = 42.16 µM BT549, IC_{50} = 48.9µM HeLa). By comparing the activities of **3d**, **3e**, **3f**, and **3g**, we can infer that the number and positions of the methoxy groups in ring C influence the anticancer activity. **3d** has one methoxy at C4', **3e** has three methoxy groups at 2',3' and 4' positions of ring C and **3g** has two methoxy groups at 3' and 4' positions of ring C (Fig. 1). They

were found to be inactive (IC_{50} > 100µM), whereas **3f** with two methoxy groups at 2' and 4' positions of ring C was found to be moderately active (IC_{50} = 61.90 µM) against BT549, (IC_{50} = 38.26 µM) against HeLa. As can be seen from Table 1 none of the synthesized molecules displayed cytotoxicity on normal cells (Supplementary Data Figs. S1-S2).

Single crystal X-ray diffraction experiments were carried out for the compounds **3h,** and **3i** (Fig. 1) and the thermal ellipsoid diagrams of the molecules are shown in **3h** and **3i** (Supplementary Data Fig. S3). Crystal data and structure refinement details are given in Table 2, and hydrogen bonds are listed in Table 3-4 for **3h** and **3i** respectively. The atomic coordinates of all the non-hydrogen atoms with their equivalent isotropic, anisotropic displacements parameters, the positional and isotropic displacement of the hydrogen atoms, the bond lengths, bond angles, and torsion angles involving all the atoms for **3h** and **3i** were given in Supplementary Data (Table S1-S8). The relevant crystallographic data for the title compound have been deposited at Cambridge Crystallographic Data Centre (CCDC) with CCDC Nos. 1552499 (**3h**) and 1552500 (**3i**).

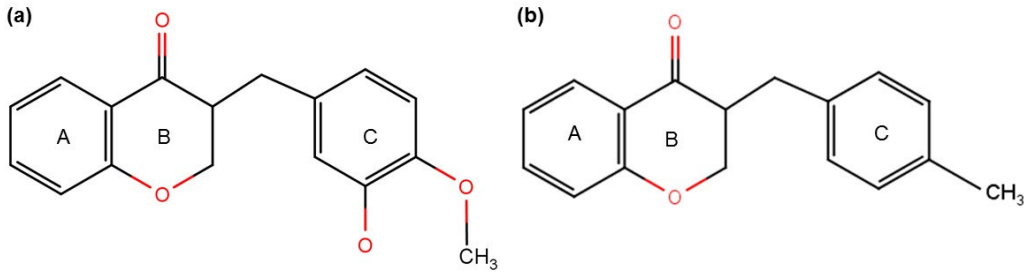

Fig. 1. Chemical diagram of **3h (a)**, and **3i (b)**

The pyranone ring has adopted the envelope conformation.[12] The ring puckering parameters q_2 = 0.2489 (7) Å, q_3 = -0.1631 (7) Å, Q_T = 0.2976 (6) Å, and φ = -126.17(15)° for **3h** are indicative of an envelope conformation. Fig. 2 shows the molecular packing features of **3h**. In the crystal, the molecules are interlinked through strong O3-H3O…O3 [symmetry ½-x, ½+y, ½-z), O3-H3O…O4 [symmetry ½-x, ½+y, ½-z) hydrogen bonds (Table 3, Fig. 2a). Also two weak C-H…O interactions (Fig. 2a) and C5'-H5'…π (C5-C10) (Fig. 2b) interactions with H…Cg – 2.94 Å [symmetry code 1-x, 1-y, -z] play a role in stabilizing the molecules. There are no π-π stacking interactions present in the structure.

Table 2

Crystal data and structure refinement for 3h and 3i.

Identification code	3h	3i
Empirical formula	$C_{17}H_{16}O_4$	$C_{17}H_{16}O_2$
Formula weight	284.30	252.30
Temperature	293(2) K	293(2) K
Wavelength	0.71075 Å	0.71075 Å
Crystal system	Monoclinic	Monoclinic
Space group	P 2_1/n	P 2_1/n
Unit cell dimensions	a = 8.581(9) Å	a = 4.6459(8) Å
	b = 6.484(6) Å	b = 26.802(4) Å
	c = 25.29(3) Å	c = 10.9485(19) Å
	β = 98.28(2) °	β = 101.876(17) °
Volume	1392(3) $Å^3$	1334.1(4) $Å^3$
Z	4	4
Density (calculated)	1.356 Mg/m^3	1.256 Mg/m^3
Absorption coefficient	0.096 mm^{-1}	0.081 mm^{-1}
F(000)	600	536
Crystal size	0.3 X 0.25 X 0.19 mm^3	0.28 X 0.20 X 0.18 mm^3
Theta range for data collection	3.167 to 25.324°.	2.434 to 26.369°.
Index ranges	-10<=h<=8, -4<=k<=7, -26<=l<=30	-5<=h<=5, -33<=k<=33, -13<=l<=13
Reflections collected	4929	14066
Independent reflections	2493 [R(int) = 0.0381]	2721 [R(int) = 0.1420]
Completeness to theta = 25.242°	98.3 %	99.9 %
Refinement method	Full-matrix least-squares on F^2	Full-matrix least-squares on F^2
Data / restraints / parameters	2493 / 0 / 207	2721 / 0 / 174
Goodness-of-fit on F^2	1.064	0.983
Final R indices[I>2sigma(I)]	R1 = 0.0690, wR2 = 0.1402	R1 = 0.0863, wR2 = 0.2388
R indices (all data)	R1 = 0.1253, wR2 = 0.1670	R1 = 0.1616, wR2 = 0.3192
Extinction coefficient	0.0032(14)	0.005(5)
Largest diff. peak and hole	0.172 and -0.207 $e.Å^{-3}$	0.281 and -0.250 $e.Å^{-3}$
CCDC	1552499	1552500

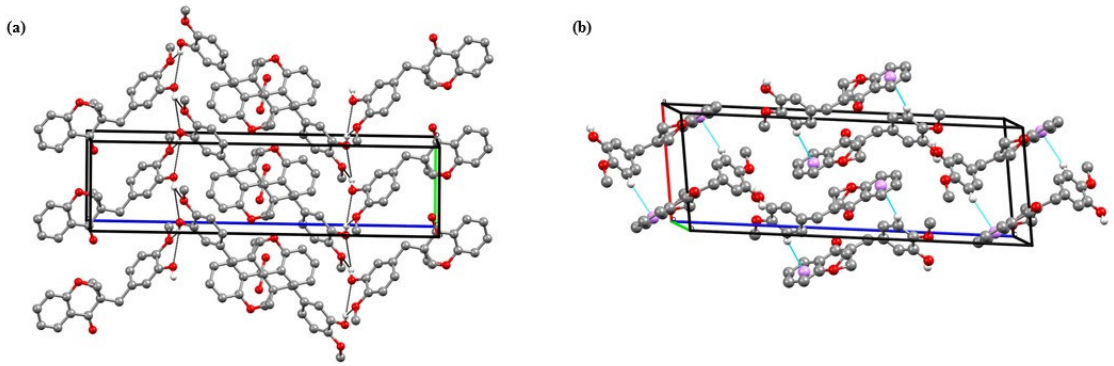

Fig. 2. The intermolecular interactions of 3h. (a) The O-H…O and (b) C-H…π hydrogen bonds are represented by dashed lines. For the clarity purpose, C-H…O hydrogen bonds and hydrogen atoms which are not involved in interactions are not shown. The O-H…O hydrogen bonds forming a network of interactions along *b* direction is evident.

Table 3

Hydrogen bonds for 3h [Å and °].

D-H...A	d(D-H)	d(H...A)	d(D...A)	<(DHA)
O(3)-H(3O)...O(3)#1	0.95(4)	2.52(4)	3.291(3)	138(3)
O(3)-H(3O)...O(4)#1	0.95(4)	1.97(4)	2.808(4)	146(4)
C(2')-H(2')...O(3)#1	0.93	2.63	3.245(4)	124.1
C(2A)-HC2A...O(2)#2	0.97	2.57	3.092(12)	114.1
C(5')-H(5')...Cg1#3	0.93	2.93	3.788(4)	153.0

Symmetry transformations used to generate equivalent atoms:

#1 -x+1/2,y+1/2,-z+1/2 #2 x,y-1,z #3 1-x,1-y,-z

The ring B in **3i** is not planar, as previously observed.[13-15] The carbon C2 has the largest offset from the plane defined by the adjacent benzene ring A. The ring puckering parameters of pyronone ring of **3i** is q_2 = 0.3829 (1) Å, q_3 = -0.2640(1) Å, Q_T = 0.4651(1) Å, and φ =-107.21(1) ° are indicative of an envelope conformation. No classical inter-or intra molecular hydrogen bonds are observed. The packing of the **3i** is stabilized into a three-dimensional network of weak C(2)-H(2B)...O(2) intermolecular interactions viewed along *a* direction, which serve to link inversion-related sheets (Fig. 3 and Table 4), which is well supported by the earlier investigations.[16]

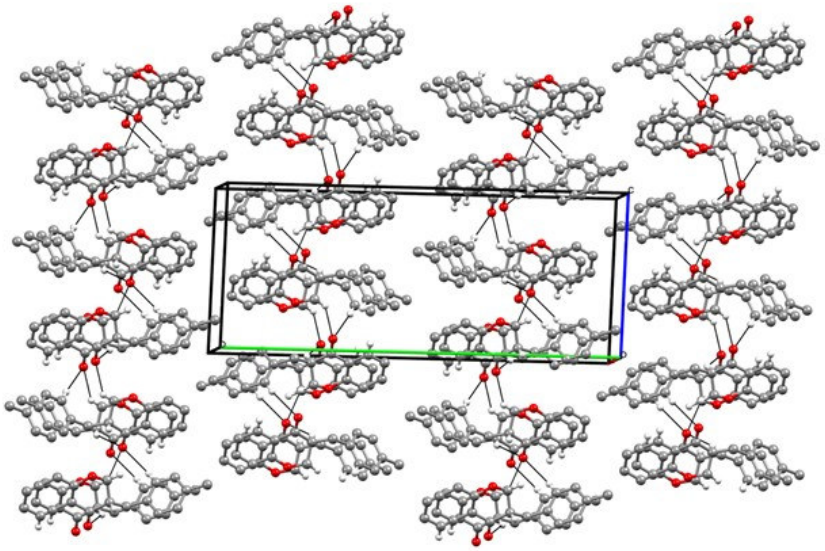

Fig. 3. The intermolecular interactions of 3i viewed along *a* direction. The dashed lines represent weak C-H…O hydrogen bonds. For the clarity purpose hydrogen atoms which are not involved in interactions are not shown. The C-H…O hydrogen bonds are forming a network of interactions along *c* direction, and overlay of molecules as sheet along *b* direction is also shown.

Table 4

Hydrogen bonds for 3i [Å and °].

D-H...A	d(D-H)	d(H...A)	d(D...A)	<(DHA)
C(2)-H(2B)...O(2)#1	0.97	2.52	3.318(4)	139.8

Symmetry transformations used to generate equivalent atoms:

#1 x-1/2,-y+1/2,z+1/2

In both the compounds, the bond lengths, bond angles are usual,[17] and all 19 common non-hydrogen atoms can be superimposed with Root Mean Square deviation (RMSD) of 0.23 Å. Similarly, the geometric parameters are comparable with the analogue structures of rac-3-(4-hydorxybenzyl)chroman-4-one,[14] and 3-(3,4-dimethoxybenzyl)chroman-4-one[15] reported earlier. It is interesting to note that C2 and C3 atoms and its relevant hydrogen atoms are also disordered in the earlier reported structure rac-3-(4-hydorxybenzyl)chroman-4-one[14] and 2-benzyl- and (E)-2-benzylidene-1-tetralones.[13] Curiously either one of these atoms is involved in stabilizing the crystal structures through weak C-H…O hydrogen bonding. Superimposition of the chroman-4-one moiety (except C2, and C3 atoms) the RMSD is varied from 0.014 Å to 0.019 Å, and C4' atom of benzyl moiety is spanning within 2.08Å (Fig. 4a). **3h** and 3-(3,4-dimethoxybenzyl)chroman-4-one structures have methoxy moieties at C4' position. While **3h** methoxy adopts a *cis* position with C5'-C4'-O4-C12 = 8.05°, 3-(3,4-dimethoxybenzyl)chroman-4-one has a dihedral angle of 165.12° for the similar bond with a methyl group is facing opposite each other (Fig. 4b). The conformation of the molecule can also be explained systematically by the dihedral angle between the planes of the two benzene rings (Fig. 1, A & C rings).[18] In the reported molecules, it is found to be 82.6(2)° for **3h**, and 69.6(2)° for **3i**. This angle is 59.1(1)° for 3-benzylidene-4-chromanone[19], 80.1(1) for rac-3-(4-hydorxybenzyl)chroman-4-one,[14] and 87.0(1) for 3-(3,4-dimethoxybenzyl)chroman-4-one molecules.[15] This shows that the substitution at ring C, in particular at C4' position plays a significant role in the conformation of the 4-chromanone molecules (Fig. 4).

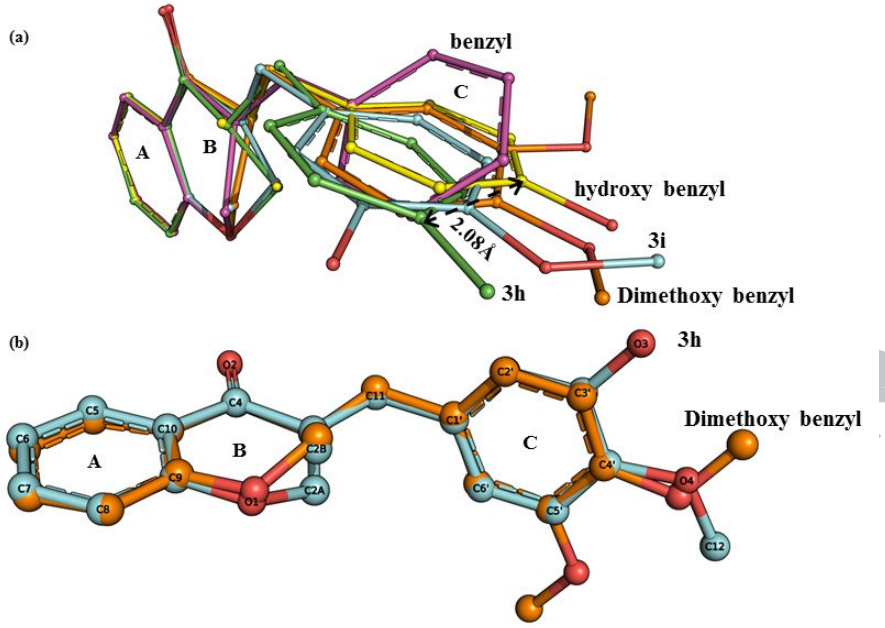

Fig. 4. Comparison of 3-benzylidene-4-chromanone molecules. 3h, 3i, 3-benzylidene-4-chromanone, dimethoxybenzyl, and hydroxybenzyl chromanone molecules are superimposed and shown in ball and stick. (a) All the atoms (except C2 and C3) in the rings A and B (are superimposed to identify the effect of various substitutions at ring C. (b) All the common atoms of **3h** (cyan) and dimethoxybenzyl (orange) molecules are superimposed. Both the molecules have overall similar conformations, and methoxy moieties at C4' position adopt opposite orientation.

Chroman-4-one derivatives are more often than not used as an inhibitor for the treatment of cancer.[20, 21] Chromone and chromanone moieties are also frequent targets for various enzymes such as HIV-1,[22] mTOR/PI3Kα,[23] mycobacterium P450 DM,[24] hepatitis C virus NS5B polymerase,[25] bovine serum albumin (BSA),[26] β-site amyloid precursor protein cleaving enzyme 1 (BACE1),[27] COX1/COX2,[28] and α-glucosidase.[29,30] In particular, benzylidenechroman-4-ones are tested as inhibitors of human monoamine oxidase isoforms A and B,[31] and its derivatives are identified as inhibitors of anticancer, anti-tubercular and antioxidant agents.[32]

On the other hand, the tumour-suppressor protein p53 is one of the primary targets for cancer therapy.[33-35] p53 is described as "the guardian of the genome" due to its role in preserving the genomic information, and it prevents cancer formation. The p53 human protein is a homotetramer comprising 4 x 393 amino acids and primarily function as a transcription

factor.[36] The p53 protein is also responsible for repairing cellular DNA, and p53 mutants are common and occur in almost 50% of all cancers. Mutations in p53, in particular at DNA binding domain destabilize the activity of p53 and leads to a narrow opening in its surface. Several mutations such as Y220C, V143A, D245S, R248Q, R249S, F270L, R273H, and R282W are reported as responsible destabilizing the function of the protein thus cause 30% - 40% of cancer mutation functions. Any small molecule that binds to these positions may reverse the stucture function relationship of this protein. Hietanen *et al*. showed that small molecules could restore the function of p53 in the nucleus of HeLa, CaSki, and SiHa cells, which leads to induction of the apoptotic death of the cells.[37] Recently Joerger *et al*. have proposed several small-molecule stabilizers for open and closed forms of the p53 cancer mutant Y220C.[36] As molecule **3h** induced cytotoxicity in HeLa cells, docking study was

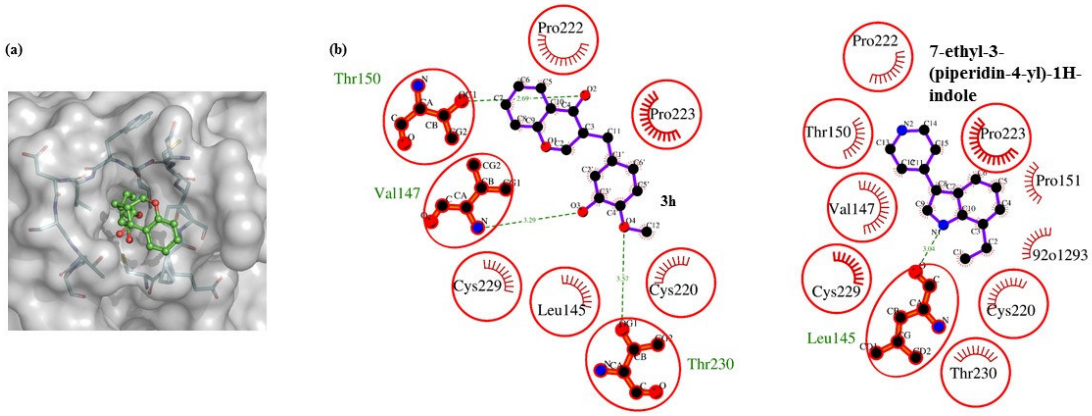

carreied out to explore the possibilites of 3-benzylchroman-4-one derivatives as inhibitors of p53 at the Y220 active site of p53. In the docking model of p53-3h, ligand **3h** is bound within the active site of Y220C of p53 and it is surrounded by the Leu145, Trp146, Val147, Asp148, Ser149, Thr150, Pro151, Cys220, Glu221, Pro222, Pro223, Asp228, Cys229, and Thr230 amino acids of p53 (Fig. 5a, Supplementary Data Table S9). All the oxygen atoms (except O1) of **3h** molecule make hydrogen bonds with Val147 (N-H…O, 3.29Å), Thr150 (O-H…O, 2.69 Å), and Thr230 (O-H…O, 3.57 Å) of p53. It also makes hydrophobic contacts (within 5 Å) with Lue145, Cys220, Pro222, Pro223, and Cys229 of p53 amino acid residues (Fig. 5b). The binding affinity of ligand **3h** for p53 (-7.0) is calculated, and the molecular interactions of the final model are compared with the crystal structure of the p53 cancer mutant Y220C (PDB id: 5AB9) crystallized with 7- ethyl-3-(piperidin-4-yl)-1H-indole (Fig. 5c). The small molecule bound with p53 structure interact with ten residues of p53. Out of these ten residues, eight residues were found to have common interactions with p53-3h docking model.

Fig. 5. Molecular interactions of 3h with p53. (a) Surface representation of p53 with 3h is shown. The amino acids in the active site are shown in stick (cyan) inside the transparent surface of p53. The 3h molecule is shown in ball and stick model and colored green (carbon). (b) *In Silico* docking results of p53 with 3h, and (c) molecular interactions of p53 crystallized with 7-ethyl-3-(piperidin-4-yl)-1H-indole (right, PDB Id: 5AB9) is shown. The p53 amino acids within 4.2Å proximity are shown, and the hydrogen bonds are depicted in dotted lines and highlighted in a green ball and stick models. The hydrophobic contacts are shown in an arc with spokes radiating towards the ligand atom in contact. Common amino acids interacting with 3h and 7-ethyl-3-(piperidin-4-yl)-1H-indole are highlighted within the circle.

Recent studies on bio-inspired catechol synthesis showed that catechol derivatives are useful building blocks for amino acids and pharmaceuticals.[38-41] The **3h** compound has a 4-chromanone moiety connected with guaiacol moiety bridged through CH_2. Guaiacol is a universal substrate for all peroxidases. A simple search of Protein Data Bank yield five structures bound with quaiacol (PDB id: 4QOQ – Bacillus pumilus catalase; PDB ids: 4A78 and 4A6Z – cytochrome c peroxidase; PDB id: 4G05 - Pleurotus eryngii versatile peroxidase; and PDB id: 3HT9 – T4 lysozyme). In the case of Bacillus pumilus catalase structure, guaiacol moiety stabilized the protein structure by reducing the disorder in the terminal residues, and guaiacol exhibited the highest occupancy than catechol. The methyl group of guaiacol moiety in **3h** is located all the way inside of the binding pocket of p53 and surround by the critical amino acids Trp146 (4.79 Å), Val147 (3.61 Å), and Cys220 (4.22 Å). It is interesting to note that Cys220 p53 mutant is one of the potential therapeutic agents and approximately 75000 tumours annually worldwide are found to have this common mutation. This mutation destabilizes the protein by 4 kcal/mol and could potentially be a target by the drug molecules.[42]

From the X-ray crystallographic structures, it is evident that benzyl moiety undergoes conformational changes based on the substitutions and molecular interactions. The **3h** molecule has three rotatable bonds in between two phyenyl rings, and it may be possible that either the amino acids of p53 or **3h** molecule may reorient and come closer than the currently proposed model and may make better contacts with Cys220 of p53 protein. As we discussed earlier, the docking model of 3h-p53 forms three hydrogen bonds, and five hydrophobic contacts studies, thus the ligand **3h** may play a significant role with the receptor protein p53. Though 3**h** molecule is different from the various small molecules proposed by Joerger *et*

al.,[33, 36] the interactions of **3h** bear a resemblance to all these molecules co-crystallized with p53. All amino acids (Leu145, Val147, Thr150, Cys220, Pro222, Pro223, and Cys229, and Thr230) except Pro151 identified in the p53-**3h** interface (Fig. 5b) plausibly play a significant role in cytotoxicity of the molecule. As we discussed earlier, p53 is a potential target for anticancer immunotherapy, and our docking results provide an eviedence that 3-benzylchroman-4-one derivatives may be poteintal inhibitors for Y220C p53.

In summary, a series of fifteen 3-benzylchroman-4-one derivatives were synthesized and characterized. 3b (3-(4-Hydroxybenzyl)-chroman-4-one) exhibited maximum cytotoxicity against BT549 cells (IC_{50} = 20.1 µM) and 3h (3-(3-Hydroxy-4-Methoxybenzyl)-chroman-4-one) against HeLa cells (IC_{50} = 20.45 µM). It was observed that 3-benzylchroman-4-one derivatives bearing OH substitution at 4'position of ring C displayed better cytotoxicity. X-ray crystallographic structures of **3h** and **3i** provided an insight to understand the role of substitution at benzyl moieties in stabilizing the structures. At the molecular level, the structures in present study resemble well with the previously known structures of 3-benzylidene-4-chromanone derivatives, but the crystal packing is different. The docking studies of 3h revealed its specificity for p53 protein as a small molecule for the Y220C mutant. These findings suggest that optimizing the structural elements of these new 3-benzylidene-4-chromanone derivatives may enhance its anticancer properties further, and provide a class of inhibitors with a plausible use in the treatment of cancer which warrants future conclusive experiments.

Conflicts of Interest: None

Acknowledgement:

We would like to acknowledge the support of Department of Science and Technology, Science and Engineering Research Board, India Grant SB/FT/LS-273/2012. Ms. Shilpa thanks, Manipal University, India for the MU Ph.D. fellowship and we would like to thank Professor Santhosh Chidangil for his encouragement and support. LS is thankful to Director, Manipal Institute of Technology and Principal Manipal College of Pharmaceutical Sciences, Manipal University for providing research facilities.

References

1. López, S. N.; Sierra, M. G.; Gattuso, S. J.; Furlán, R. L.; Zacchino, S. A. *Phytochemistry* **2006,** *67*, 2152.
2. Ata, A.; Gale, E. M.; Samarasekera, R. *Phytochem. Lett.* **2009,** *2*, 106.
3. Du Toit, K.; Elgorashi, E. E.; Malan, S. F.; Drewes, S. E.; van Staden, J.; Crouch, N. R.; Mulholland, D. A. *Bioorg. Med. Chem.* **2005,** *13*, 2561.
4. Fusi, F.; Ferrara, A.; Koorbanally, C.; Crouch, N. R.; Mulholland, D. A.; Sgaragli, G. *J. Pharm. Pharmacol.* **2008,** *60*, 489.
5. Gaspar, A.; Matos, M. J.; Garrido, J.; Uriarte, E.; Borges, F. *Chem. Rev.* **2013,** *114*, 4960.
6. Kang, L.; Zhao, H.; Chen, C.; Zhang, X.; Xu, M.; Duan, H. *Int. Immunopharmacol.* **2016,** *38*, 246.
7. Hur, S.; Lee, Y. S.; Yoo, H.; Yang, J.-H.; Kim, T.-Y. *J. Dermatol. Sci.* **2010,** *59*, 163.
8. Dang, N. H.; Chung, N. D.; Tuan, H. M.; Hiep, N. T.; Dat, N. T. *Chem. Pharm. Bull.* **2017,** *65*, 204.
9. Bandgar, B. P.; Gawande, S. S.; Bodade, R. G.; Totre, J. V.; Khobragade, C. N. *Bioorg. Med. Chem.* **2010,** *18*, 1364.
10. Ahmed, N.; van Lier, J. E. *J. Chem. Res.* **2006,** *2006*, 584.
11. Jaspal, S.; Grover, S. K. *Indian J. Chem., Sect B* **2004,** *43B*, 1782.
12. Cremer, D.; Pople, J. A. *J. Am. Chem. Soc.* **1975,** *97*, 1354.
13. Valkonen, A.; Laihia, K.; Kolehmainen, E.; Kauppinen, R.; Perjési, P. *Struct. Chem.* **2012,** *23*, 209.
14. Shalini, S.; Girija, C.; Simon, L.; Srinivasan, K.; Venkatesha, T. *Acta Crystallogr., Sect. E: Struct. Rep. Online* **2013,** *69*, o1011.
15. Shalini, S.; Girija, C.; Simon, L.; Srinivasan, K.; Venkatesha, T.; Jotani, M. *Acta Crystallogr., Sect. E: Struct. Rep. Online* **2013,** *69*, o241.
16. Desiraju, G. R.; Steiner, T. *The weak hydrogen bond: in structural chemistry and biology*: Oxford University Press on Demand, 2001.
17. Allen, F. H.; Kennard, O.; Watson, D. G.; Brammer, L.; Orpen, A. G.; Taylor, R. *J. Chem. Soc., Perkin Trans. 2* **1987**, *0*, S1.
18. Abdul Ajees, A.; Manikandan, S.; Raghunathan, R. *Acta Crystallogr., Sect. E* **2002,** *58*, o535.
19. Katrusiak, A.; Ratajczak-Sitarz, M.; Kałuski, Z.; Orlov, V. *Acta Crystallogr., Sect. C: Struct. Chem.* **1987,** *43*, 103.
20. Seifert, T.; Malo, M.; Kokkola, T.; Engen, K.; Fridén-Saxin, M.; Wallén, E. A.; Lahtela-Kakkonen, M.; Jarho, E. M.; Luthman, K. *J. Med. Chem.* **2014,** *57*, 9870.
21. Emami, S.; Ghanbarimasir, Z. *Eur. J. Med. Chem.* **2015,** *93*, 539.
22. Ungwitayatorn, J.; Wiwat, C.; Samee, W.; Nunthanavanit, P.; Phosrithong, N. *J. Mol. Struct.* **2011,** *1001*, 152.
23. Zhu, W.; Chen, C.; Sun, C.; Xu, S.; Wu, C.; Lei, F.; Xia, H.; Tu, Q.; Zheng, P. *Eur. J. Med. Chem.* **2015,** *93*, 64.
24. Ayati, A.; Falahati, M.; Irannejad, H.; Emami, S. *Daru, J. Pharm. Sci.* **2012,** *20*, 46.
25. Wei, Y.; Li, J.; Qing, J.; Huang, M.; Wu, M.; Gao, F.; Li, D.; Hong, Z.; Kong, L.; Huang, W. *PloS one* **2016,** *11*, e0148181.
26. Ashok, D.; Madhuri, E. V.; Sarasija, M.; Kanth, S. S.; Vijjulatha, M.; Alaparthi, M. D.; Sagurthi, S. R. *RSC Adv.* **2017,** *7*, 25710.
27. Seong, S. H.; Ali, M. Y.; Kim, H.-R.; Jung, H. A.; Choi, J. S. *Bioorg. Med. Chem.* **2017,** *25*, 3964.
28. Abolhasani, H.; Dastmalchi, S.; Hamzeh-Mivehroud, M.; Daraei, B.; Zarghi, A. *Med. Chem. Res.* **2016,** *25*, 858.
29. Takao, K.; Yamashita, M.; Yashiro, A.; Sugita, Y. *Chem. Pharm. Bull.* **2016,** *64*, 1203.
30. Uesawa, Y.; Sakagami, H.; Kagaya, H.; Yamashita, M.; Takao, K.; Sugita, Y. *Anticancer Res.* **2016,** *36*, 5803.
31. Desideri, N.; Bolasco, A.; Fioravanti, R.; Proietti Monaco, L.; Orallo, F.; Yáñez, M.; Ortuso, F.; Alcaro, S. *J. Med. Chem.* **2011,** *54*, 2155.

32. Das, U.; Lorand, T.; Dimmock, S. G.; Perjesi, P.; Dimmock, J. R. *J. Enzyme Inhib. Med. Chem.* **2015,** *30*, 259.
33. Joerger, A. C.; Bauer, M. R.; Wilcken, R.; Baud, M. G.; Harbrecht, H.; Exner, T. E.; Boeckler, F. M.; Spencer, J.; Fersht, A. R. *Structure* **2015,** *23*, 2246.
34. Parrales, A.; Iwakuma, T. *Front. Oncol.* **2015,** *5*, 288.
35. Semenova, E. A.; Nagel, R.; Berns, A. *Genes Dev.* **2015,** *29*, 1447.
36. Joerger, A. C.; Fersht, A. R. *Cold Spring Harbor Perspect. Biol.* **2010,** *2*, a000919.
37. Hietanen, S.; Lain, S.; Krausz, E.; Blattner, C.; Lane, D. P. *Proc. Natl. Acad. Sci. U. S. A.* **2000,** *97*, 8501.
38. Wu, Q.; Yan, D.; Chen, Y.; Wang, T.; Xiong, F.; Wei, W.; Lu, Y.; Sun, W.-Y.; Li, J. J.; Zhao, J. *Nat. Commun.* **2017,** *8*, 14227.
39. Xiong, F.; Lu, L.; Sun, T.-Y.; Wu, Q.; Yan, D.; Chen, Y.; Zhang, X.; Wei, W.; Lu, Y.; Sun, W.-Y. *Nat. Commun.* **2017,** *8,* 15912.
40. Chen, Y.; Wang, D.; Duan, P.; Ben, R.; Dai, L.; Shao, X.; Hong, M.; Zhao, J.; Huang, Y. *Nat. Commun.* **2014**, *5*, 4610.
41. Wu, Q.; Chen, Y.; Yan, D.; Zhang, M.; Lu, Y.; Sun, W.Y.; Zhao, J. *Chem. Sci.* **2017***, 8*, 169.
42. Wiman, K. G. *Oncogene* **2010,** *29*, 4245.